



Biocompatible nanocarriers of bioactive flavonoid naringin: Design, formulation, and comprehensive characterization

Rituparna Chaki^{1*}, Souvik Basak¹, Arpana Sharma², Vilas D. Nasare², Nilanjan Ghosh³, Subhash C. Mandal³

¹Dr. B.C. Roy College of Pharmacy and Allied Health Sciences, Durgapur, India.

²Department of Pathology and Cancer Screening, Chittaranjan National Cancer Institute, Kolkata, India.

³Department of Pharmaceutical Technology, Jadavpur University, Kolkata, India.

ARTICLE HISTORY

Received on: 03/10/2024

Accepted on: 18/03/2025

Available Online: 05/07/2025

Key words:

Anti-inflammatory, chitosan, entrapment, nanocarriers, naringin, solubility.

ABSTRACT

Naringin (NAR), a citrus flavonoid has been reported to have anti-inflammatory, antitumor, antiviral, antiadipogenic, and cardioprotective qualities. However, because of its poor aqueous solubility, therapeutic applications of NAR are limited. The present research involves development of nanocarriers of NAR using biocompatible natural polymer chitosan and tripolyphosphate using ionic gelation method. Surface morphology studies indicated the structure of the prepared nanocarriers with an entrapment of more than 80% and appreciable average size range of around 100 nm. Drug release studies suggested that the drug released at a controlled manner with around of 65% over a period of 6 hours with a burst release of around 20% in the first hour. 3-(4, 5-dimethylthiazol-2-yl)-2, 5-diphenyl tetrazolium bromide test using HEK 293 cells demonstrated that highest concentration of NAR loaded nanocarriers (100 μ M) showed optimal viability and cells were not harmed by nanocarriers. *In-vivo* anti-inflammatory activity study suggested that prepared formulation (50 mg/kg) significantly reduced development of carrageenan induced paw edema, comparable with diclofenac treated rats (10 mg/kg) but significantly enhanced for rats treated with NAR only (50 mg/kg). Together, the results suggested that chitosan based nanocarriers could be an efficient tool to deliver naringin thus ensuring better bioavailability to enhance its therapeutic potential.

INTRODUCTION

Numerous research-based studies have shown the important therapeutic benefits of phytochemicals. Despite being researched to treat a number of complex human illnesses, phyto drugs have a number of limitations that keep them from realizing their full potential as active pharmaceutical ingredients. Low permeability, low water solubility, high toxicity, instability, low bioavailability, are some of these limiting factors which make the formulation development of phytodrugs [1,2]. Drug delivery for conditions like chemotherapy, diabetes, and cancer treatment may be improved by the use of nanocarriers for active phytoconstituents, which have demonstrated encouraging

results in this regard. Utilizing this approach, some of its disadvantages might be eliminated and a stable pharmaceutical product made entirely of phytochemicals trapped in nanocarriers could be developed. When appropriately adapted, enabling the administration through nanocarriers may increase the drug's systemic availability and desired target action. [3].

Many fruits, including citrus fruits, tomatoes, and bergamot, contain flavanones, also known as flavonoids, like naringenin. Additionally, it exists as glycosides, most notably as naringin (NAR). This phytochemical is thought to have anti-inflammatory, antitumor, antiviral, antiadipogenic, cardioprotective properties [4]. A study has suggested the protective activity of NAR against the Lipopolysaccharide-induced apoptosis in PC12 cells [5]. The findings by Zhao *et al.* [6] indicated that NAR inhibits inflammation and apoptosis in endothelial cells by controlling the Hippo-YAP Pathway. The cardio protecting mechanism and effect were summarized by Heidary Moghaddam *et al.* [7]. Another

*Corresponding Author

Rituparna Chaki, Dr. B.C. Roy College of Pharmacy and Allied Health Sciences, Durgapur, India. E-mail: rituparna.chaki@gmail.com

research has elucidated the anti-degenerative properties for cartilage and bones [8]. Bajgai *et al.* [9] comprehensive analysis from 2024 provides insight on how sepsis-induced multiple organ dysfunction can be alleviated. However, it has also been reported to have low bioavailability because of poor aqueous solubility and hence several researchers have suggested various ways to improve its delivery for effective therapeutic benefits [10–13].

In this work, the biocompatible natural polymer chitosan was used to load naringin into nanocarriers. Chitosan is a natural polycationic polymer that can attach to mucous membranes and increase absorption in the gastrointestinal tract by loosening the tight connections between epithelial cells. In recent years, chitosan has been widely researched due to its exceptional ability to serve as a nanocarrier material [14]. They are affordable, have a large range of drug compatibility, and allow for sustained delivery [15]. As a crosslinking agent, sodium tripolyphosphate (TPP) is utilized [16]. When combined with chitosan, sodium TPP works wonders as a crosslinking agent. By forming stable nanopockets, they prolong the release of the medicine and help it travel to its target site of action. In order to examine naringin's bioavailability and possible anti-inflammatory effects, the current study employs the ionotropic gelation process to create chitosan-TPP cross-linked nanoparticles (NPs). The prepared NPs were characterized for drug loading, size distribution, surface morphology and release studies. Rats were used in *in vivo* anti-inflammatory study, and HEK 293 cells were used in an *in vitro* cytotoxicity assay to confirm non-toxicity to normal cell lines.

MATERIALS AND METHODS

Materials

Naringin, chitosan ($\geq 75\%$ deacetylated), and dimethyl sulfoxide (DMSO) was purchased from Sigma Aldrich. Glacial acetic acid and sodium TPP were purchased from HiMedia Laboratories, dialysis membrane of MW cut off, 12,400 was purchased from Sigma Aldrich. All other chemicals used for the research study were of laboratory grade. 3-(4, 5-dimethylthiazol2-yl)-2, 5-diphenyl tetrazolium bromide (MTT) used for cytotoxicity studies was purchased from Sigma Aldrich. All chemicals for cell culture analysis were cell culture grade.

Method of preparation of naringin loaded chitosan (NLC) nanocarriers

NLC nanocarriers were created via the ionic gelation technique. Acetic acid 1% (v/v) was used to prepare chitosan solution. The chitosan solution was continuously mixed as naringin was added dropwise. Over the course of 2 hours, while stirring continuously, the chitosan solution was gradually combined with the sodium TPP solution, which was kept at 4°C [17,18]. Chitosan was used at different concentrations (0.5–2 mg/ml). Drug was incorporated into the NLC nanocarriers at a concentration of 0.25 mg/ml. Amount of TPP used was optimized at 0.5 mg/ml which was fixed for all formulations. To find the best formulation, a range of TPP volumes, drug

Table 1. Impact of chitosan concentration increase on ZP, PDI, and particle size.

Formulation	Chitosan (mg/ml)	Particle Size (nm)	PDI	ZP (mV)	%LC	%EE
NLC1	0.5	91.92	0.2	25.6	25	75.25
NLC2	1	130.3	0.25	28.1	16.67	82.41
NLC3	1.5	215.21	0.43	32.2	12.5	65.5
NLC4	2	470.5	0.33	36.6	10	58.8

concentrations, and polymer concentrations were tested and the best formulations were tabulated in Table 1.

Characterizations of NLC nanocarriers

Fourier Transform Infrared study (Fourier Transform Infrared study) spectrum analysis

The FTIR studies were carried out for NAR, chitosan and the NLC carriers under identical conditions to detect any possible interactions between the components that may lead to precipitation of the drug. It was carried out by mixing the sample with potassium bromide to form a pellet and scanning the sample over a wavelength from 4,000 to 400 cm^{-1} .

X-ray crystallography analysis

The X-ray crystallography of NAR, blank NLC carriers, and NLC carriers containing NAR was performed by Cu K α radiation, at a voltage of 40 kV and 30 mA. The angle of scanning was adjusted from 5° to 70°, and the scanned rate was 4°/min.

Entrapment efficiency (EE)

After ultra-centrifuging NLC samples, the sediment and supernatant fluids were gathered. Absorbance was then measured with a UV spectrophotometer in the supernatant for the unentrapped drug concentration [19]. EE and drug loading capacity (LC) was determined using to equation:

$$EE = (\text{Amount of NAR encapsulated into formulation}) / (\text{Amount of the total NAR added}) \times 100$$

$$LC = (\text{Weight of NAR in formulation}) / (\text{Total weight of the formulation}) \times 100$$

Physical characterization

Using a Zetasizer Nano Instrument, dimension of the prepared NLCs was determined. A suitable concentration of NLC was agitated at 100 rpm and maintained at 37°C in distilled water. After being allowed to dry at ambient temperature, the NLC nanocarriers' structure was examined using a scanning electron microscope (SEM) and transmission electron microscope (TEM) to study their surface properties. For TEM, a drop of diluted NLC suspension was deposited on a film-coated copper grid, stained with one drop of 2% (w/v) aqueous solution of phosphotungstic acid, and then allowed to dry for contrast enhancement.

In vitro release study

Naringin, equivalent to 5 mg, was filled into a dialysis bag and placed in phosphate buffer solution (pH 7.4, 50 ml). The

beaker was magnetically stirred at 100 rpm while being kept at $37^{\circ}\text{C} \pm 0.5^{\circ}\text{C}$. UV spectrophotometry was used to measure the absorbance after 5 ml samples were taken out and replaced with new buffer solution at predefined intervals [19].

Cytotoxicity study

Cell line and reagent: The National Collection of Cell Sciences, Pune is the source of human derived embryonic kidney HEK 293 cells. The cells were kept in modified Eagle's medium supplemented with 2 mM glutamine, 10% fetal bovine serum that has been heat-inactivated, 1% penicillin-streptomycin solution, and 5% CO_2 at 37°C in a humidified atmosphere.

Cytotoxicity assay: The MTT technique was employed to assess the vitality of cells *in vitro* [20]. In 96-well plates, 8,000 HEK 293 cells were planted each well and allowed to attach for a full day. The following day, the used media was removed and replaced with new glutamine medium containing varying concentrations of NAR (6.25, 12.25, 25, 50, and 100 μM) for 24 hours. After the target time point was reached, 20 μl of MTT dye (5 mg/ml) dissolved in phosphate buffer saline was added to each well, and the incubator was left in the dark for 4 hours at 37°C . After carefully extracting the media containing MTT dye, 100 μl of DMSO was given to each well to dissolve the formazan crystal. The wells were then left for 10 minutes at room temperature in the dark. Each well's absorbance was calculated using a micro-plate reader at 570 nm [21].

$$\text{Cell viability (\%)} = \frac{A_{\text{treatment}} - A_{\text{blank}}}{A_{\text{control}} - A_{\text{blank}}} \times 100\%$$

Anti-inflammatory activity

Male and female Wistar rats weighing between 100 and 150 g were employed to assess the formulation's anti-inflammatory properties. Before the trials began, the rats were given a balanced food and unlimited access to water for approximately 2 weeks while they adjusted to the laboratory environment. Every animal was housed at $24^{\circ}\text{C} \pm 2^{\circ}\text{C}$ with a relative humidity of $60\% \pm 5\%$ and exposed to a 12/12 hour light/dark cycle by the appropriate institutional review body. Animal experiments in the present study and the study protocol was reviewed and approved by Institutional Animal Ethical Committee (IAEC) of Dr B C Roy College of Pharmacy and AHS (Reference No: BCRC/IAEC/2/2019).

The paw edema model induced by the phlogistic agent, carrageenan, was employed to evaluate the anti-inflammatory activity of prepared NLC carriers. Rats were divided into five groups ($n = 6$), and were given one of the following treatments: Group 1: distilled water + carrageenan; Group 2: blank formulation + carrageenan; Group 3: free NAR (50 mg/kg, p.o) + carrageenan; Group 4: NLC (50 mg/kg, p.o) + carrageenan; and Group 5: diclofenac (10 mg/kg, p.o.) + carrageenan.

A single hour following the administration of the various agents, the right hind paw's sub-plantar tissue was injected with 0.1 ml carrageenan (1% w/v in saline) to induce edema. After administering carrageenan, paw volume was measured plethysmographically at 0th, 1st, 2nd, 3rd, 4th, and 6th hours [22,23]. The % of inhibition was calculated using the following formula:

$$\% \text{ Inhibition} = \frac{(\text{Increase in paw edema}_{\text{control}} - \text{Increase in paw edema}_{\text{treated}})}{\text{Increase in paw edema}_{\text{control}}} \times 100$$

RESULTS AND DISCUSSION

Synthesis of NLC nanocarriers

Naringin loading into chitosan is facilitated by electrostatic attraction, hydrogen bonding, and hydrophobic interactions. Chitosan, a hydrophilic organic polymer, has a positive charge due to protonation in an acidic environment. NAR with hydroxyl and glycoside groups, can create hydrogen bonds with chitosan's amino groups, keeping it stable inside the matrix. Hydrophobic pockets in chitosan can capture lipophilic NAR molecules and load them into the chitosan network. Stabilization of NAR within the chitosan matrix may be due to weak van der Waals forces, which facilitate non-covalent interactions over short distances. Chitosan's gel-like network in aqueous environments allows it to form complexes with various drug molecules, including NAR. Naringin can be encapsulated within the chitosan matrix by mixing it with chitosan. When chitosan is dissolved in an acidic solution, it swells and turns cationic. When NAR is added to the chitosan solution, it interacts with the chitosan through hydrogen bonding and electrostatic interactions [24–26].

Characterization and optimization of NLC nanocarriers

FTIR spectrum analysis: The FTIR spectra of NAR revealed two prominent peaks corresponding to the wavenumber of the hydroxyl group at wave number regions 1,664.02 and 3,330.14 cm^{-1} . The compound's structure and the outcome of the infrared spectroscopy (IR) spectrum assessment for NAR matched, confirming the result. The IR spectra of chitosan show several absorption bands corresponding to its functional groups. A broad peak around 3,431.78 cm^{-1} is observed due to the stretching vibrations of hydroxyl (O-H) groups, often associated with hydrogen bonding. The N-H stretching of primary amine groups is also present, overlapping with the O-H band. The C-H stretching vibrations of the chitosan polymer backbone appear at 2,925.98 and 2,881.09 cm^{-1} . The most prominent peaks are the amide I band at 1,642.03 cm^{-1} , which corresponds to the stretching of carbonyl bonds from residual N-acetyl groups in partially deacetylated chitosan. The C-N stretching of amine groups shows characteristic peaks around 1,381.03 and 1,320.80 cm^{-1} . The FTIR spectra of the chitosan nanoparticle verified the presence of the chitosan's important peak. The tip of the peak in chitosan NPs has shifted to 3,427.85 cm^{-1} , indicating an increase in hydrogen bonding; in TPP. The FTIR spectrum of a chitosan nanoparticle loaded with NAR revealed a characteristic peak change from 1,664.02 to 1,642.09 cm^{-1} , indicating that NAR had been incorporated into the chitosan nanoparticle without any possible interaction that may lead to precipitation of the drug (Fig. 1a). All functional groups have been mentioned in Table 2.

The Drug-polymer (chitosan) characterization has further been done with the help of X ray diffraction spectra of the compound together with the polymer (chitosan). The drug diffractogram (Fig. 1b (A)) shows that most of the peaks are sharp and crisp indicating that the drug bears mostly crystalline nature

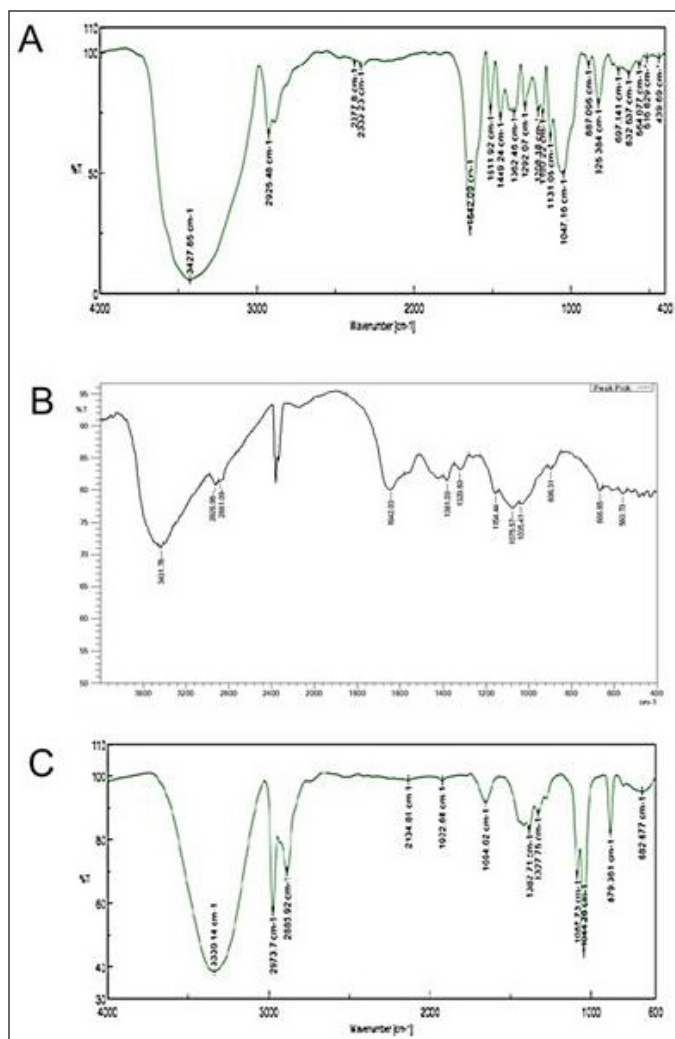


Figure 1. (A) FTIR spectra of Naringin (B) FTIR spectra of Chitosan (C) FTIR spectra of NLC formulation.

in its form. However, the chitosan peaks (Fig. 1b (B)) revealed suppressed and interspersed peaks suggesting its amorphous nature. Interestingly the formulation diffractogram (Fig. 1b (C)) reveals high resemblance with the polymer suggesting that the polymer has been in the outer core of the formulation while the drug has been entrapped inside the polymeric core. Moreover, the height of the peaks of the formulation at specific 2θ values are found to be quite different from that of the polymer as well as the drug suggesting that there have been change of crystallinity or arrangement of atoms in specific planes of the formulation (or Drug-Polymer complex). Now this could be a plausible inference that the change of crystallinity or atomic arrangement (marked by the change of intensity of peaks) might be due to the drug-polymer interaction that has incurred to the value addition of the complex.

In order to produce NLC nanocarriers with the desired size range, the formulation process variables were optimized. The zeta potential (ZP), particle size, entrapment efficiency, and polydispersity index (PDI) were all significantly impacted by each of these process variables. Table 1 illustrates how increasing the chitosan concentration affects ZP, PDI, and average particle size. Particle size average, PDI, and ZP all grew progressively with rise in the level of chitosan. The particle size of the prepared NPs ranged from 91.92–470.5 nm which suggested that the size of the NPs increased as the concentration of chitosan increased from 0.5 to 2 mg/ml. The ZP of the NPs varied around +30mV which indicated a good stability for the prepared NPs. Figure 2 depicts the particle size of one of the optimized formulations. Furthermore, increasing the chitosan content from 0.5 to 1 mg/ml resulted in a noticeable improvement in the nanoparticles' encapsulation efficiency. However, an increase in concentration beyond 1.5 mg/ml further showed a decrease in the drug entrapment, possibly because of inconsistent interaction of chitosan with TPP. At

Table 2. FTIR analysis grouping.

Peaks (wavenumber in cm ⁻¹)	Naringin	Chitosan	Naringin-chitosan nanoparticle
1,664.02 cm ⁻¹	-C=O stretch of chalcoprynone moiety of the flavonoid		
3,330.14 cm ⁻¹	-OH stretch the flavonoid		
3,431.78 cm ⁻¹		-OH stretch of the polymer	
2,925.98 cm ⁻¹		The C-H stretching vibrations of the chitosan polymer backbone	
2,881.09 cm ⁻¹		The C-H stretching vibrations of the chitosan polymer backbone	
1,642.03 cm ⁻¹		the stretching of carbonyl bonds from residual N-acetyl groups in partially deacetylated chitosan	
1,381.03 and 1,320.80 cm ⁻¹		The C-N stretching of amine groups	
3,427.85 cm ⁻¹			-OH peak shift to chitosan nanoparticle
1,664.02 to 1,642.09 cm ⁻¹			-C=O stretch of chitosan nanoparticle

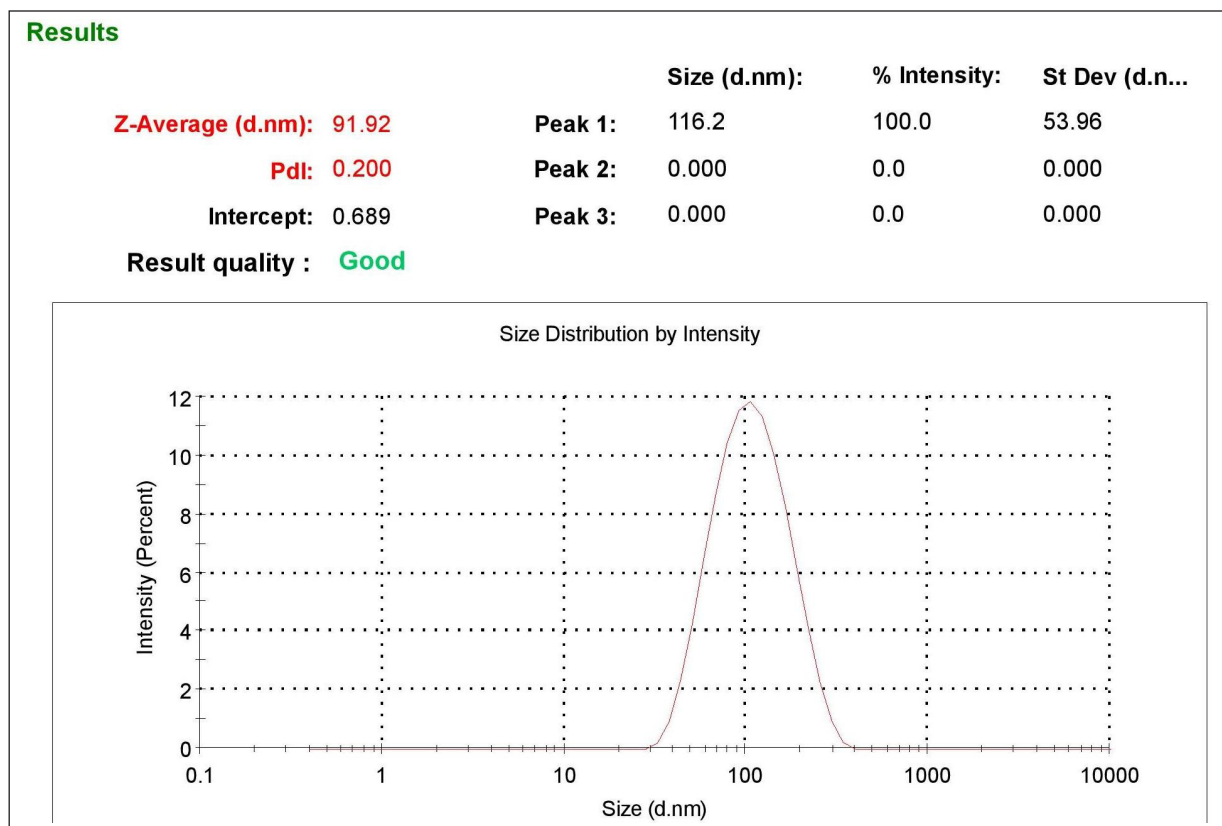


Figure 2. Particle size distribution of prepared NLCs.

higher chitosan concentrations, this could be explained by the formation of more chitosan chains per volume [27].

The NLC nanocarriers were spherical, well-separated, uniformly distributed, and had a rough surface and morphology, according to the morphology studies (Fig. 3a). Figure 3b exhibits well dispersed nanocarriers of chitosan through TEM under a magnification of 200× which corroborates with the results obtained by SEM.

In vitro release studies: Drug release studies indicated that a controlled release of approximately 65% of the drug could be achieved over 6 hours. All of the formulations, however, displayed a 15% burst release within the first hour. It is possible that the surface of the nanocarriers contained drug molecules, which would account for the initial fast release. The drug embedded in the matrix was the cause of the consistent and slow release of NAR from NPs. Results clearly suggests that with an increase in chitosan concentration there is a reduction in the rate of drug release from the nanocarriers (Fig. 4a) [28]. In order to know the mechanism of drug release from the formulations, the release data were treated according to zero-order, first-order, Higuchi, Hixson-Crowell and Korsmeyer Peppas model. None of the formulations followed complete zero order release pattern. The release profiles could be best expressed by Higuchi's plot as it exhibited high linearity ($R^2 > 0.98$). Thus, the mechanism of drug release from nanocarriers can be described by diffusion controlled mechanism with a burst release. The release exponent n was found to be less than 0.45 in the Korsmeyer-Peppas model for all formulations, which

indicates Fickian diffusion, meaning drug release is controlled primarily by a diffusion mechanism without significant polymer relaxation or swelling. Since the Higuchi model also describes diffusion-driven release, the high linearity observed in the Higuchi plot ($R^2 > 0.98$) aligns well with the Fickian diffusion mechanism. This confirms that the drug release from the formulation follows a diffusion-controlled process without significant contributions from polymer erosion or swelling (Fig. 4b).

The linearity of the assay method was calculated by estimating the R^2 value of the curve. The R^2 estimated as 0.993 (Table 2) suggested a good linearity of the calibration curve. The limit of detection (LOD) was determined as 91.9059 $\mu\text{g}/\text{ml}$ and limit of quantification (LOQ) as 278.5027 $\mu\text{g}/\text{ml}$ (Table 3). The accuracy (percentage recovery) varied from 99.96%–103.79% (Table 4 and Table 5).

MTT assay for assessing cytotoxicity

MTT test showed that the NAR did not damage the cells. The absorbance values increased at NAR doses in certain concentrations of NLC, but were non-significant as compared to untreated cells ($p > 0.05$). Figure 5a and b represents cell viability analysis. For viability, HEK 293 cells were treated with the indicated concentrations (0–100 μM) of NAR for 24 hours and MTT assay was performed to check cell viability. The data are presented as means of triplicate samples for each treatment and values given as mean \pm SEM. Statistical analysis was performed by students

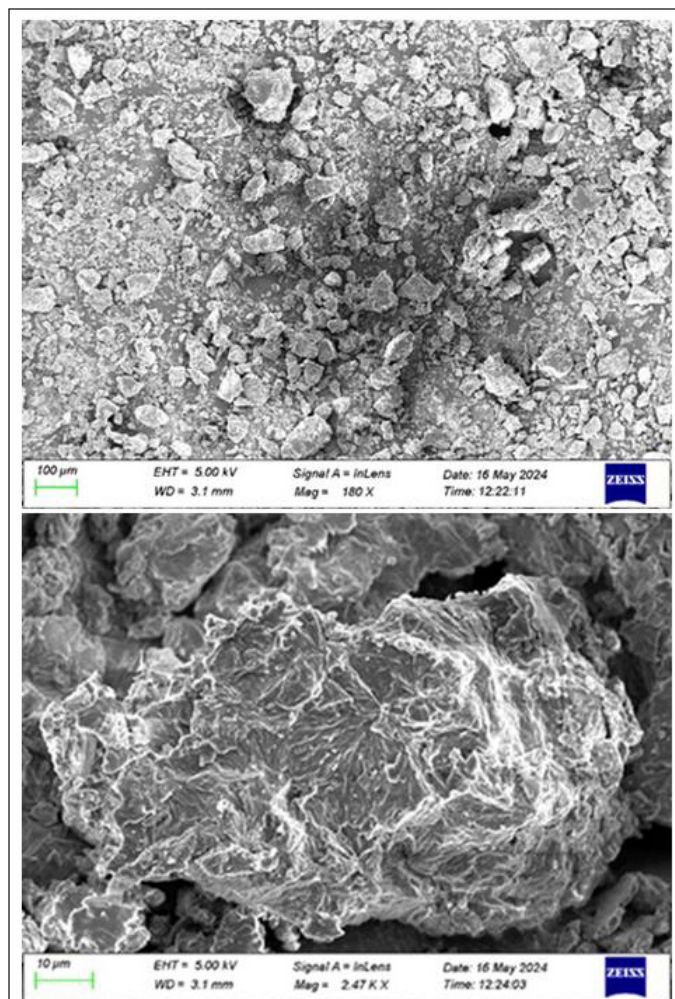


Figure 3a. Morphology study using scanning electron microscopy (SEM).

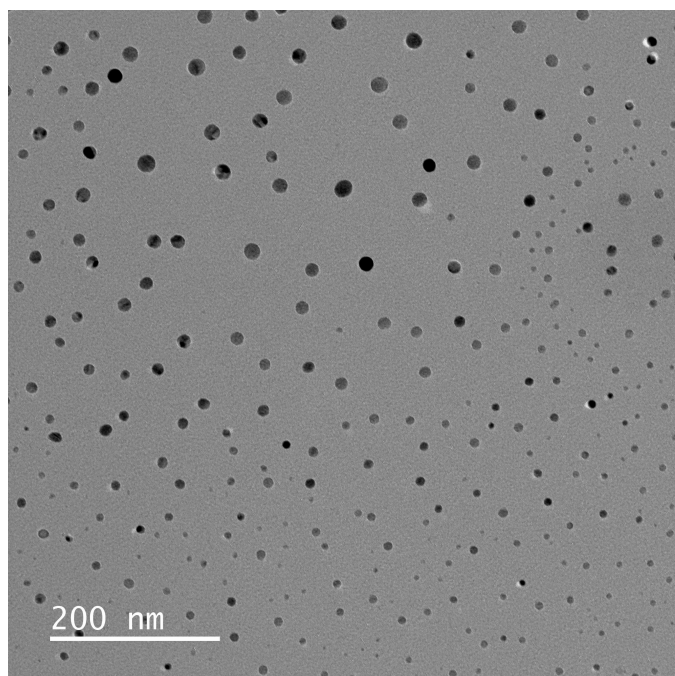


Figure 3b. Surface morphology study using transmission electron microscopy.

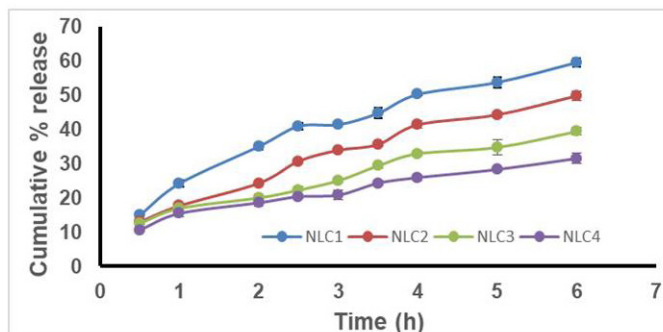


Figure 4a. Release profile of NLC formulations.

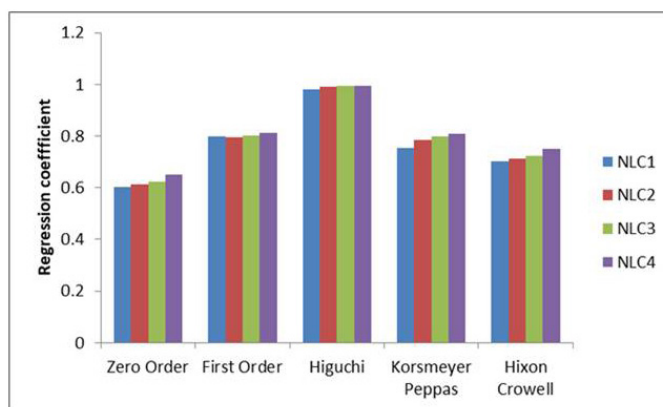


Figure 4b. Release kinetics of NLC formulations.

Table 3. Table for validation parameters.

Parameter	Value
Linearity	$R^2 = 0.993$
LOD (3.3 σ /s)	91.9059 $\mu\text{g/ml}$
LOQ (10 σ /s)	278.5027 $\mu\text{g/ml}$

σ = Standard deviation of the intercept; s = slope of the regression (fitting) curve.

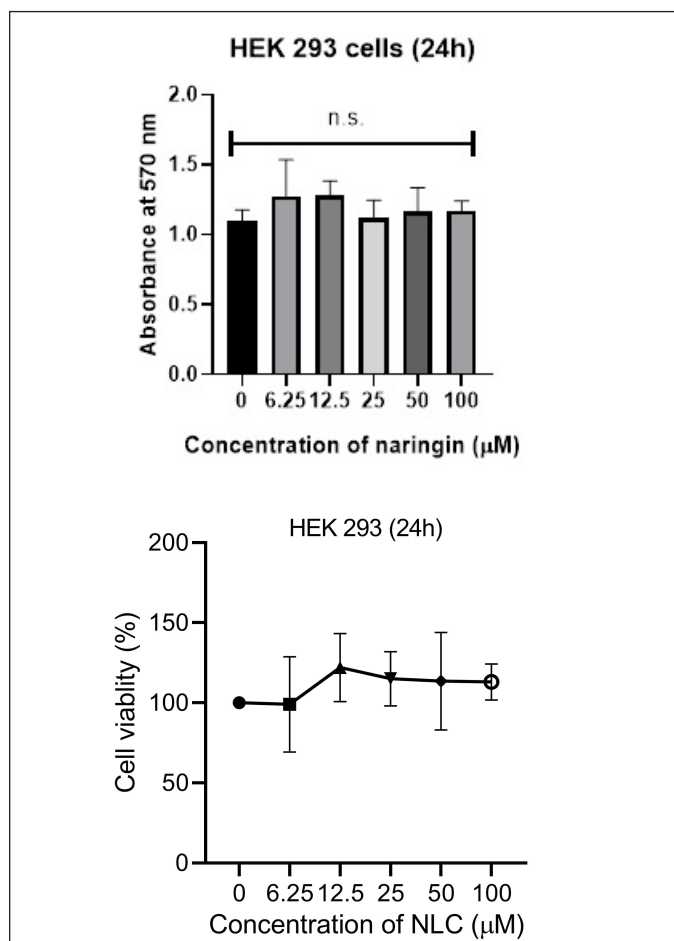
t-test; Bars = SE; n.s. = non-significant. The cells exhibited optimal viability at the highest concentration of NLC (100 μM) and 0.5% chitosan, it was concluded that the cells were healthy safe at these concentrations which are nontoxic to the normal cell's growth and viability. Additionally, we saw no morphological alterations in the HEK 293 cells following the medication treatment as in comparison with the untreated group. Figure 6 represents images of morphological changes of untreated control and NLC-treated HEK 293 cells observed under an inverted light microscope (20 \times magnification) and no morphological changes are observed [29].

Anti-inflammatory activity

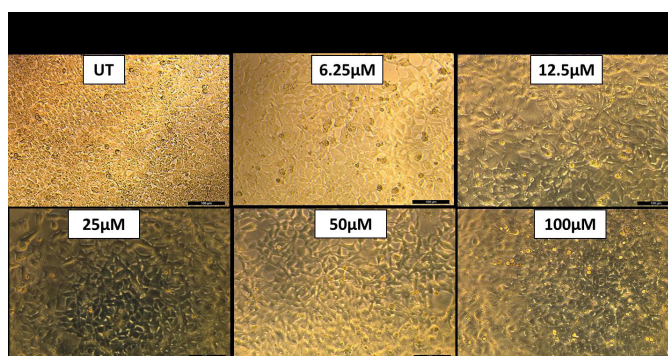
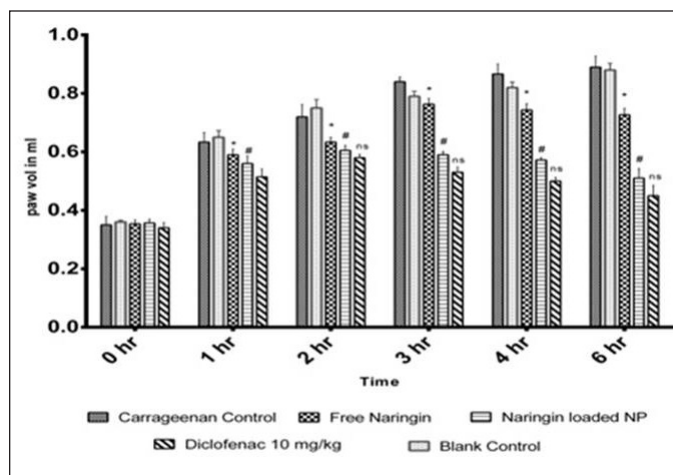
The posterior intraplantar left paw volume in the vehicle treated group grew gradually after receiving an injection of 0.1 ml of carrageenan (1% w/v), peaking at 0.89 ± 0.03 ml after 6 hours. The % inhibition of paw edema for the NAR treated group was found to be 9.52%, 13.95%, and 19.10% at the 3, 4 and 6 hours mark, respectively. At the 3, 4, and 6 hours

Table 4. Estimation of accuracy (recovery).

Taken concentration (µg/ml)	Absorbance			Recovered conc1 (µg/ml)	Recovered conc 2 (µg/ml)	Recovered conc 3 (µg/ml)	Average	SD
	Abs 1	Abs 2	Abs 3					
40	0.6321	0.6785	0.6624	39.10377	43.48113	41.96226	41.51572	2.222581
50	0.7345	0.749	0.7587	48.76415	50.13208	51.04717	49.98113	1.14897
60	0.8667	0.8989	0.8478	61.23585	64.27358	59.45283	61.65409	2.43744

**Figure 5.** Graphs showing MTT assay for cytotoxicity analysis on HEK cells at different naringin concentrations against control.

marks, the percentage suppression of paw edema for the NAR loaded nanoparticle group was found to be 297.66%, 33.72%, and 42.67%, respectively. With $p > 0.05$, result was found to be similar to that of the diclofenac treated group with one way ANOVA, accompanied by Dunnett's test. The % inhibition for the diclofenac treated group was found to be 36.90%, 41.86% and 46.94% at the 3, 4 and 6 hours mark, respectively. **Figure 7** explains NLC's anti-inflammatory properties assessed over time using pleurisy induced by carrageenan. Every value is presented as Average \pm SEM ($n = 6$); * indicates a significant difference ($p < 0.05$) between the free NAR group and the conventional control group. Diclofenac treated; # denotes

**Figure 6.** Microscopic images of no morphological changes of HEK cells at different naringin concentrations of NLC.**Figure 7.** NLC's anti-inflammatory properties assessed over time using pleurisy induced by carrageenan.

$p < 0.05$, significant difference compared amongst free naringin and naringin loaded nanoparticle group; when comparing the naringin-loaded nanoparticle group to the standard control group (treated with Diclofenac), ns indicates $p > 0.05$, non-significant (by one way ANOVA followed by Dunnett's test).

The acute anti-inflammatory efficacy of NLC has been assessed using pleurisy caused by carrageenan. Carrageenan is utilized in the screening process for anti-inflammatory compounds because it is a phlogistic agent and creates a severe inflammatory response when injected locally into a rat's paw. Carrageenan-induced inflammation occurs in three distinct phases: the first is characterized by the release of serotonin and

Table 5. Calculation of percentage recovery of the study.

Taken concentration (µg/ml)	Recovered concentration	Percentage recovery
40	41.51572327	103.7893082
50	49.98113208	99.96226415
60	61.65408805	102.7568134

histamine; the second is brought about by kinin production, bradykinin being the most prominent; and the third is regulated by prostaglandins. NLC inhibited the development of rat paw edema considerably during the middle phase of carrageenan-induced inflammation, and this effect was more pronounced during the third phase. This suggests that the anti-inflammatory properties of NLC may be mediated by reduction of prostaglandin activity in conjunction with the effects of vasoactive molecules (histamine, serotonin, and kinins) [30–33].

The putative clinical benefits of naringin are restricted due to its poor aqueous solubility, low bioavailability and high hepatic first-pass metabolism [4]. The naringin embedded in the NLC nanocarriers exhibited higher anti-inflammatory activity as compared to naringin can be attributed to several key factors observed in similar studies on naringin and other flavonoid-loaded NPs. First, NPs significantly enhance the bioavailability of poorly soluble compounds like naringin, ensuring a higher concentration of the active compound at the site of inflammation. Furthermore, naringin is released gradually and under control by NPs, resulting in a protracted therapeutic action that guarantees steady anti-inflammatory benefits throughout time. Furthermore, because of their tiny size, NPs enhance cellular absorption and make it easier for naringin to enter target immune cells like macrophages, where it can more successfully inhibit inflammatory reactions. Additionally, naringin is shielded by NPs from enzymatic breakdown in the blood or gastrointestinal tract, increasing the amount of the active ingredient that reaches the site of inflammation intact. This protective mechanism, coupled with improved pharmacokinetics, such as prolonged half-life and reduced clearance, further enhances the anti-inflammatory potential of naringin NPs [34–39].

CONCLUSION

In this study, we successfully prepared and evaluated chitosan-based nanocarriers encapsulating the citrus flavonoid naringin. The outcomes showed that the nanocarriers had advantageous physicochemical characteristics, such as a controlled release profile, appreciable encapsulation efficiency, and an ideal particle size. The efficient and repeatable synthesis technique used produced NPs with homogeneous morphology, as demonstrated by analyses using particle size analysis, SEM and TEM analysis. Naringin was found to be released from chitosan nanocarriers over an extended period of time, according to *in vitro* release studies, indicating the possibility of long-term therapeutic benefits. Furthermore, the anti-inflammatory potential of the naringin-loaded nanocarriers was significantly enhanced in comparison to free NAR, indicating that the encapsulation process preserved and possibly amplified the bioactivity of the flavonoid.

Overall, the study's results demonstrate the intriguing possibilities of chitosan-based nanocarriers as a NAR delivery system, providing increased bioactivity and prolonged release. These characteristics make them a promising candidate for additional research and development in the management of pathologic conditions where the therapeutic potential of NAR might be beneficial. To confirm these results and investigate the complete therapeutic potential of NLC nanocarriers, future research can be conducted on *in vivo* assessments and clinical trials.

AUTHOR CONTRIBUTIONS

All authors made substantial contributions to conception and design, acquisition of data, or analysis and interpretation of data; took part in drafting the article or revising it critically for important intellectual content; agreed to submit to the current journal; gave final approval of the version to be published; and agree to be accountable for all aspects of the work. All the authors are eligible to be an author as per the International Committee of Medical Journal Editors (ICMJE) requirements/guidelines.

FUNDING

There is no funding to report.

CONFLICTS OF INTEREST

The authors report no financial or any other conflicts of interest in this work.

ETHICAL APPROVALS

The study protocol was approved by the Institutional Animal Ethical Committee (IAEC) of Dr. B.C. Roy College of Pharmacy and Allied Health Sciences, India (Reference No: BCRCP/IAEC/2/2019).

DATA AVAILABILITY

All the data is available with the authors and shall be provided upon request.

PUBLISHER'S NOTE

All claims expressed in this article are solely those of the authors and do not necessarily represent those of the publisher, the editors and the reviewers. This journal remains neutral with regard to jurisdictional claims in published institutional affiliation.

USE OF ARTIFICIAL INTELLIGENCE (AI)-ASSISTED TECHNOLOGY

The authors declares that they have not used artificial intelligence (AI)-tools for writing and editing of the manuscript, and no images were manipulated using AI.

REFERENCES

1. Teeranachaideekul V, Müller RH, Junyaprasert VB. Encapsulation of ascorbyl palmitate in nanostructured lipid carriers (NLC): effects of formulation parameters on physicochemical stability. *Int J Pharm.* 2007;340(1–2):198–206. doi: <https://doi.org/10.1016/j.ijpharm.2007.03.034>

2. Siddiqui IA, Sanna V. Impact of nanotechnology on the delivery of natural products for cancer prevention and therapy. *Mol Nutr Food Res.* 2016;60(6):1330–41. doi: <https://doi.org/10.1002/mnfr.201500928>
3. Rahman HS, Othman HH, Hammadi NI, Yeap SK, Amin KM, Samad NA, *et al.* Novel drug delivery systems for loading of natural plant extracts and their biomedical applications. *Int J Nanomedicine.* 2020;15:2439–83. doi: <https://doi.org/10.2147/IJN.S246498>
4. Chen R, Qi QL, Wang MT, Li QY. Therapeutic potential of naringin: an overview. *Pharm Biol.* 2016;54(12):3203–10. doi: <https://doi.org/10.1080/13880209.2016.1216133>
5. Wang H, Xu YS, Wang ML, Cheng C, Bian R, Yuan H, *et al.* Protective effect of naringin against the LPS-induced apoptosis of PC12 cells: implications for the treatment of neurodegenerative disorders. *Int J Mol Med.* 2017;39(4):819–30. doi: <https://doi.org/10.3892/ijmm.2017.2884>
6. Zhao H, Liu M, Liu H, Suo R, Lu C. Naringin protects endothelial cells from apoptosis and inflammation by regulating the Hippo-YAP pathway. *Biosci Rep.* 2020;40(3):BSR20193431. doi: <https://doi.org/10.1042/BSR20193431>
7. Heidary Moghaddam R, Samimi Z, Moradi SZ, Little PJ, Xu S, Farzaei MH. Naringenin and naringin in cardiovascular disease prevention: a preclinical review. *Eur J Pharmacol.* 2020;887:173535. doi: <https://doi.org/10.1016/j.ejphar.2020.173535>
8. Gan J, Deng X, Le Y, Lai J, Liao X. The development of naringin for use against bone and cartilage disorders. *Molecules.* 2023;28(9):3716. doi: <https://doi.org/10.3390/molecules28093716>
9. Bajgai B, Suri M, Singh H, Hanifa M, Bhatti JS, Randhawa PK, *et al.* Naringin: a flavanone with a multifaceted target against sepsis-associated organ injuries. *Phytomedicine* 2024;130:155707. doi: <https://doi.org/10.1016/j.phymed.2024.155707>
10. Tang W, Wei Y, Lu W, Chen D, Ye Q, Zhang C, *et al.* Fabrication, characterization of carboxymethyl konjac glucomannan/ovalbumin-naringin nanoparticles with improving *in vitro* bioaccessibility. *Food Chem X.* 2022;16:100477. doi: <https://doi.org/10.1016/j.fochx.2022.100477>
11. Im AE, Eom S, Seong HJ, Kim H, Cho JY, Kim D, *et al.* Enhancement of debitterness, water-solubility, and neuroprotective effects of naringin by transglucosylation. *Appl Microbiol Biotechnol.* 2023;107(20):6205–17. doi: <https://doi.org/10.1007/s00253-023-12692-6>
12. Ge X, Jiang F, Wang M, Chen M, Li Y, Phipps J, *et al.* Naringin@Metal-Organic framework as a multifunctional bioplatfrom. *ACS Appl Mater Interfaces.* 2023;15(1):677–83. doi: <https://doi.org/10.1021/acsami.2c18503>
13. Lee J, Kim K, Son J, Lee H, Song JH, Lee T, *et al.* Improved productivity of naringin oleate with flavonoid and fatty acid by efficient enzymatic esterification. *Antioxidants (Basel).* 2022;11(2):242. doi: <https://doi.org/10.3390/antiox11020242>
14. Jaferník K, Ładniak A, Blicharska E, Czarnek K, Ekiert H, Wiącek AE, *et al.* Chitosan-based nanoparticles as effective drug delivery systems: a review. *Molecules.* 2023;28(4):1963. doi: <https://doi.org/10.3390/molecules28041963>
15. Gulbake A, Jain SK. Chitosan: a potential polymer for colon-specific drug delivery system. *Expert Opin Drug Deliv.* 2012;9(6):713–29. doi: <https://doi.org/10.1517/17425247.2012.682670>
16. Özbaş-Turan S, Akbuğa J. Plasmid DNA-loaded chitosan/TPP nanoparticles for topical gene delivery. *Drug Deliv.* 2011;18(3):215–22. doi: <https://doi.org/10.3109/10717544.2011.555596>
17. Hoang NH, Le Thanh T, Sangpueak R, Treekoon J, Saengchan C, Thepbandit W, *et al.* Chitosan nanoparticles-based ionic gelation method: a promising candidate for plant disease management. *Polymers (Basel).* 2022;14(4):662. doi: <https://doi.org/10.3390/polym14040662>
18. Kumar S, Dilbaghi N, Saharan R, Bhanjana G. Nanotechnology as emerging tool for enhancing solubility of poorly water-soluble drugs. *BioNanoSci.* 2012;2:227–50. doi: <https://doi.org/10.1007/s12274-012-0131-x>
19. Joshi G, Kumar A, Sawant K. Enhanced bioavailability and intestinal uptake of gemcitabine HCl loaded PLGA nanoparticles after oral delivery. *Eur J Pharm Sci.* 2014;60:80–9. doi: <https://doi.org/10.1016/j.ejps.2014.04.003>
20. Md S, Alhakamy NA, Aldawsari HM, Asfour HZ. Neuroprotective and antioxidant effect of naringenin-loaded nanoparticles for nose-to-brain delivery. *Brain Sci.* 2019;9(11):275. doi: <https://doi.org/10.3390/brainsci9110275>
21. Hussain RF, Nouri AME, Oliver RTD. A new approach for measurement of cytotoxicity using colorimetric assay. *J Immunol Methods* 1993;160:89–96. doi: [https://doi.org/10.1016/0022-1759\(93\)90011-1](https://doi.org/10.1016/0022-1759(93)90011-1)
22. Mandal SC, Maity TK, Das J, Saba BP, Pal M. Anti-inflammatory evaluation of *Ficus racemosa* Linn. leaf extract. *J Ethnopharmacol.* 2000;72:87–92. doi: [https://doi.org/10.1016/S0378-8741\(00\)00215-4](https://doi.org/10.1016/S0378-8741(00)00215-4)
23. Mandal SC, Lakshmi SM, Kumar CK, Sur TK, Boominathan R. Evaluation of anti-inflammatory potential of *Pavetta indica* Linn. leaf extract (family: Rubiaceae) in rats. *Phytother Res.* 2003;17(8):817–20. doi: <https://doi.org/10.1002/ptr.1177>
24. Agnihotri SA, Mallikarjuna NN, Aminabhavi TM. Recent advances on chitosan-based micro- and nanoparticles in drug delivery. *J Control Release.* 2004;100(1):5–28. doi: <https://doi.org/10.1016/j.jconrel.2004.08.010>
25. Sajjan P, Lingaraj L, Pujar M, Anandasadagopan SK. Chitosan nanoparticles as drug delivery systems: a review. *J Pharm Sci Res.* 2016;8(1):56–67.
26. Yadav M, Mishra P, Mishra SK. Naringin: a potential natural product in pain management. *Ther Adv Endocrinol Metab.* 2018;9(3):1–10. doi: <https://doi.org/10.1177/2042018818778296>
27. Al-Nemrawi NK, Alsharif SS, Dave RH. Preparation of chitosan-TPP nanoparticles: the influence of chitosan polymeric properties and formulation variables. *Int J Appl Pharmaceutics.* 2018;10(5):60–5. doi: <https://doi.org/10.22159/ijap.2018v10i5.27577>
28. Herdiana Y, Wathoni N, Shamsuddin S, Mughtaridi M. Drug release study of the chitosan-based nanoparticles. *Heliyon.* 2021;8(1):e08674. doi: <https://doi.org/10.1016/j.heliyon.2021.e08674>
29. Ramezani MR, Naderi-Manesh H, Rafieepour H. Cytotoxicity assessment of a gold nanoparticle-chitosan nanocomposite as an efficient support for cell immobilization: comparison with chitosan hydrogel and chitosan-gelatin. *Biocell.* 2014;38(1):11–6.
30. Ismail OI, Abidemi JA, Olufunmilayo OA. Analgesic and anti-inflammatory activities of *Cnestis ferruginea* Vahl ex DC (Connaraceae) methanolic root extract. *J Ethnopharmacol.* 2011;135:55–62. doi: <https://doi.org/10.1016/j.jep.2011.02.009>
31. Bamgbose SOA, Noamesi BK. Studies on cryptolepine II: inhibition of carrageenan-induced oedema by cryptolepine. *Planta Med.* 1981;42:392–6. doi: <https://doi.org/10.1055/s-2007-971624>
32. Lo TN, Almeida AP, Beaven MA. Dextran and carrageenan evoke different inflammatory responses in rat with respect to composition of infiltrates and effect of indomethacin. *J Pharmacol Exp Ther.* 1982;221:261–7.
33. Wang Y, Karmakar T, Ghosh N, Basak S, Sahoo NG. Targeting mangiferin-loaded N-succinyl chitosan-alginate grafted nanoparticles against atherosclerosis – A case study against diabetes-mediated hyperlipidemia in rats. *Food Chem.* 2022;370:131376. doi: <https://doi.org/10.1016/j.foodchem.2022.131376>
34. Zhang X, Liu Y, Wang J, Chen Q, Li Z. Nanoparticle delivery of naringin enhances anti-inflammatory effect in animal models. *J Nanomedicine.* 2021;16(2):142–50. doi: <https://doi.org/10.2147/IJN.S282892>
35. Patel R, Mehta T, Shah S, Desai P. Flavonoid-loaded nanoparticles for anti-inflammatory therapy: a comparative study. *Drug Deliv Lett.* 2019;10(2):89–95. doi: <https://doi.org/10.2174/2210303109666190308094259>

36. Singh A, Gupta N, Sharma R, Vashishta R. Enhanced cellular uptake and anti-inflammatory efficacy of naringin nanoparticles. *Mol Pharmacol.* 2020;17(4):225–33. doi: <https://doi.org/10.1124/mol.118.113217>
37. Gupta A, Kumar P, Aggarwal S, Khurana N. Protection of naringin from degradation using nanoparticles. *J Drug Deliv Sci Technol.* 2022;65:102–10. doi: <https://doi.org/10.1016/j.jddst.2021.102110>
38. Ahmed S, Alam M, Khan A, Hussain Z. Curcumin and flavonoid nanoparticles for targeted anti-inflammatory treatment. *J Mol Med.* 2020;98(5):311–20. doi: <https://doi.org/10.1007/s00109-019-01817-w>
39. Sharma D, Bansal R, Thakur V, Chawla P. Pharmacokinetic advantage of naringin nanoparticles in inflammation models. *Nanomedicine (Lond).* 2021;15(3):200–10. doi: <https://doi.org/10.2217/nnm-2020-0173>

How to cite this article:

Chaki R, Basak S, Sharma A, Nasare VD, Ghosh N, Mandal SC. Biocompatible nanocarriers of bioactive flavonoid naringin: Design, formulation, and comprehensive characterization. *J Appl Pharm Sci.* 2025;15(08):117–126. DOI: 10.7324/JAPS.2025.222894